American Mineralogist, Volume 91, pages 394–399, 2006

The crystal structure of a second antigorite polysome (m = 16), by single-crystal synchrotron diffraction

GIAN CARLO CAPITANI[1,*] AND MARCELLO MELLINI[2]

[1]Dipartimento Geomineralogico, Via Orabona 4, 70125, Bari, Italy
[2]Dipartimento di Scienze della Terra, Via Laterina 8, 53100 Siena, Italy

ABSTRACT

A model for the modulated crystal structure of an antigorite polysome with m = 16 (where m is related to the number of tetrahedra spanning a wavelength along **a**) was refined by single-crystal synchrotron diffraction data in $C2/m$, using crystals coexisting with the m = 17 polysome from Val Malenco, Italy, which was previously determined structurally. Lattice parameters [a = 81.664(10), b = 9.255(5), c = 7.261(5) Å, β = 91.409(5)°] were determined using a single-crystal diffractometer equipped with an area detector at the Desy synchrotron (Hamburg). The structure was solved by direct methods, and the model refined using 19 222 symmetry-related reflections. The final $R_{4\sigma}$ factor was 0.0951, calculated for 7246 reflections.

The structure of the m = 16 antigorite polysome strongly resembles that of the m = 17 polysome. A continuous, wavy octahedral sheet is linked to a tetrahedral sheet, reversing its polarity through sixfold tetrahedral and eightfold tetrahedral rings. The half-wave has a curvature radius of 80.1 Å. Polyhedral geometry, ditrigonalization angles, and interlayer O-O distances are similar in the two polysomes. The only differences concern the number of tetrahedra for the m = 16 polysome (an even number which leads to symmetric half-waves) and the periodic **b**/2 shift involving the eightfold rings (to produce the doubling of the a parameter and a C-centered cell).

Keywords: Antigorite, structure, synchrotron, polysomatism

INTRODUCTION

The modulated crystal structure of the common m = 17 antigorite polysome (m being the number of tetrahedra spanning a wavelength along the **a** axis) was recently determined using three-dimensional X-ray diffraction data (Capitani and Mellini 2004). The structure [Pm space group; a = 43.505(6), b = 9.251(1), c = 7.263(1) Å, β = 91.32(1)°] involves a wave-like 1:1 layer, curled on the **b**-axis and modulated along [100]. When observed along [010], sixteen octahedra form a continuous octahedral (**O**) sheet with flex lines midway; seventeen tetrahedra (**T**) link the **O**-sheet at the concave sides, eight of them forming a "short" half-wave, and nine, with opposite polarity, forming a "long" half-wave (see Capitani and Mellini 2004, Fig. 1). The **T**-sheet contains 6-membered tetrahedral rings, as in an ideal serpentine such as lizardite, which reverse polarity via alternating "6-reversals" and "8-reversals". The 6-reversals consist of 6-membered tetrahedral rings; four tetrahedra point along **c*** and two point along **–c***. The 8-reversals consist of 8-membered tetrahedral rings (four tetrahedra point along **c*** and four along **–c***), coupled along [010] with 4-membered tetrahedral rings (two tetrahedra point along **c*** and two along **–c***), as shown in Figure 2 of Capitani and Mellini (2004).

The m = 17 antigorite structure was first envisaged by L. Onsager (as reported by Robinson and Shaw 1952). Kunze (1958) performed the first two-dimensional structural determination, obtaining the correct configuration of the **T**-sheet, but deriving an **O**-sheet biased by offsets at reversal lines that produced unusual Mg coordinations (tetragonal pyramids and three-sided prisms). After electron and X-ray diffraction studies, Uehara and Shirozu (1985) proposed a model (with atomic positions given in Uehara 1998) that more correctly resemble the structure later experimentally determined for the m = 17 polysome by Capitani and Mellini (2004). Therefore, the structure of the m = 17 polysome [and, in general, the structural topology of the "odd" (m = $2n$ + 1) antigorite structures] seem now defined.

Different models, none yet fully validated, have been proposed for the "even" (m = $2n$, where n is an integer) antigorites. Kunze (1961) proposed a $P2/m$ model with only 4- and 8-membered tetrahedral rings at reversal lines, and offsets in the **O**-sheet, thus creating tenfold Mg coordinations. Uehara and Shirozu (1985) corrected that model, inserting periodic faults with **b**/2 shifts. Every second 8-reversal is transformed into a 6-reversal, the octahedral offsets disappear, and the original P-lattice transforms to a C-centered lattice. Using high-resolution transmission electron microscopy (HRTEM), Dódony et al. (2002) proposed a model with two tetrahedral 6-reversals and only one octahedral offset (with Mg still in anomalous coordination) per unit cell. Conversely, Capitani and Mellini (2005), after HRTEM examination of polysomatic faults, supported the model of Uehara and Shirozu (1985).

It is now largely documented that any structural analysis of antigorite shows many different defects, namely (001) twinning, b/3 stacking disorder, and polysomatic faults (e.g., Spinnler 1985; Mellini et al. 1987; Otten 1993; Viti and Mellini 1996). Even a highly crystalline sample (Mg159) shows many defects (Capitani

* E-mail: g.capitani@geomin.uniba.it

and Mellini 2004, 2005; this study). After examination of more than one hundred crystals from sample Mg159, we found that the m = 17 polysome is the most common, but a few m = 16 crystals were also found. We now report the results of the crystal structure analysis of the m = 16 polysome, using single crystal, synchrotron diffraction data.

Crystal data

The single crystals used in this study come from the same 150 μm granulometric fraction (sample Mg159) separated by Peretti (1988) and used previously to obtain the m = 17 structure. Several crystals were embedded and polished for microprobe analyses (for details see Capitani and Mellini 2004). Recalculation by imposing the anionic contents of the $M_{2.813}T_2O_5(OH)_{3.625}$ stoichiometry of the m = 16 polysome gives an average (eleven point analyses) formula of $(Mg_{2.634}Fe_{0.102}Al_{0.044}Cr_{0.014}Ni_{0.003}Mn_{0.002})_{\Sigma=2.800}(Si_{1.968}Al_{0.032})_{\Sigma=2}O_5(OH)_{3.625}$, to be compared with $(Mg_{2.638}Fe_{0.102}Al_{0.047}Cr_{0.014}Ni_{0.003}Mn_{0.002})_{\Sigma=2.808}(Si_{1.971}Al_{0.029})_{\Sigma=2}O_5(OH)_{3.647}$, for the m = 17 polysome. The latter was recalculated from the data of Capitani and Mellini (2004) for sake of consistency and to fix minor shortcomings in the original calculations.

More than 100 crystals were examined by X-ray oscillation photographs, and the most promising crystals were also examined by Weissenberg techniques. Several crystals were selected for data collection by area detector diffractometers, using both conventional and synchrotron sources. Most of the crystals have cell constants consistent with the m = 17 structure (Pm space group; Capitani and Mellini 2004). A few crystals were unique. One of these (Mg159-11) has lattice parameters a = 41.096(6), b = 9.255(2), c = 7.261(7) Å, α = 90.000(7), β = 88.600(8), γ = 83.500(8)°, which transform to a = 81.664(10), b = 9.255(5), c = 7.261(5) Å, α = 90, β = 91.409(5)°, γ = 90° by the matrix $(2\bar{1}0/1\bar{1}0/00\bar{1})$.

Structural analysis

Diffraction intensities were collected at the F1 line of the Desy synchrotron (Hamburg), using a Huber 4-circle diffractometer equipped with a SMART CCD detector and a crystal-to-detector distance of 10.0 cm. A total of 5800 frames were collected, with ω = 0.3°. Counting times from 15 to 25 s per frame were used. Data reduction was performed with the SAINT+ v. 6.02 software (Bruker AXS-9/19/01). Raw intensity data were corrected for absorption using the SADABS v. 2.03 program (Sheldrick 1996).

A total of 19 526 reflections (symmetry related and/or multiply collected) were obtained to 2θ = 56.20°. A set of 4234 independent reflections resulted after merging in the 2/m Laue group, with an internal discrepancy factor of R_{int} = 0.069.

The structure was determined by the SIR-97 direct methods (Altomare et al. 1999), which defined the entire octahedral sheet and most of the tetrahedral sheet. Fourier syntheses and least-squares refinement with the SHELX-97 program (Sheldrick 1997), were used to locate the remaining tetrahedra (T) and basal (B) oxygen atoms at reversal lines, where the situation was complex, owing to polysomatic disorder. However, important ΔF residual maxima, shifted by **b**/3 with respect to the basic T-atoms, were present at this stage.

We introduced two different scale factors for reflections with $k = 3n$ and $k \neq 3n$ (where n is an integer). This led to a significant improvement of the refinement. Although reduced, the Fourier residua did not disappear completely, indicating that they are not spurious peaks but rather structure-related images of polytypic faults. Thus, two partial structures of T and B atoms were introduced with shifts of ±**b**/3 with respect to the basic structure, with occupancy constrained to one. The basic structure accounted for 82% of the diffracting volume, whereas 10% are shifted by –**b**/3 and 8% by +**b**/3.

Finally, the polysomatic disorder suggested by residual maxima close to the sheet reversals was modeled by introducing two additional disordered T-sites. The entire occupancy of the disorder related T-sites was restrained to 1.0, obtaining about 16% of faulted positions.

Hydrogen atoms were introduced at calculated positions with their x and y coordinates constrained to those of the bonded oxygen atoms, and with the z coordinates allowed to vary with a restraint on the O-H distances of 1.0 Å. Iron replacement for magnesium was not refined, because this caused instability in the refinement. As the introduction of anisotropic thermal motion did not improve the refinement and caused an additional instability, the model was refined isotropically, introducing twelve overall anisotropic parameters, using the HOPE instruction in the SHELX-97 program; this significantly lowered the R-factors and still producing physically reliable thermal motions. Two thermal parameters were refined for the hydrogen atoms, one common to the intralayer "inner" hydrogen atoms and one common to interlayer "outer" hydrogen atoms.

During the refinement, reflections were weighted according to the reciprocal of the squared standard deviations. Soft restraints were used for M-O and T-O bond distances. The final discrepancy R-factor was 0.0951 for 7246 non-merged reflections with $F_{obs} > 4\sigma(F_{obs})$. Approximately 305 independent parameters were allowed to vary during the final refinement cycles. Additional crystal and refinement data are reported in Table 1. Final atomic positional and displacement parameters in Table 2. Observed and calculated structure factors are provided on request[1].

Results

Structural topology

The topology of the m = 16 antigorite structure closely recalls the main features of the m = 17 polysome. When observed along [010], a regular and continuous **O**-sheet, consisting of 15 octahedra, extends pseudo-sinusoidally along [100] (cf., Fig. 1 with Fig. 1 in Capitani and Mellini 2004). Flex lines occur every 7.5 octahedra (namely, in the center of the M1 polyhedron and between two symmetry-related M8 polyhedra) rather than every 8 octahedra as in the m = 17 polysome. The continuous **T**-sheet links the concave side of the **O**-sheet, inverting polarity every eight tetrahedra. Although both the m = 16 and m = 17 polysomes contain apparently similar sine-like waves, these have different symmetric properties. The two half-waves are symmetry related

Table 1. Crystal data and structure refinement for the m = 16 antigorite Mg159

Ideal formula	$Mg_{45}Si_{32}O_{80}(OH)_{58}$
Wavelength	0.71069 Å
Space group	$C2/m$
Unit cell dimensions	a = 81.664(10) Å
	b = 9.255(5) Å
	c = 7.261(5) Å
	β = 91.409(5)°
Volume	5486(5) Å^3
Crystal size	160 x 60 x 30 μm^3
R_{int}/Reflections	0.0690*/19526
Data/restraints/parameters	19222/240/305
Goodness-of-fit on F^2	0.982
$R_{4\sigma}$ [$F > 4\sigma(F)$]/observed	0.0951/7593
R_{all}/all	0.2231/19222
R_1 after merging/merged	0.1454/4234

*The data set used in the refinement was reduced independently for reflections with $k = 3n$ and $k \neq 3n$. This implies a different intensity rescaling for the two intensity groups, thus impeding a reliable calculation of R_{int}. The above value refers to the same data extraction after simultaneous reduction of the entire data set.

[1] Deposit item AM-06-008, observed and calculated factors. Deposit items are available two ways: For a paper copy contact the Business Office of the Mineralogical Society of America (see inside front cover of recent issue) for price information. For an electronic copy visit the MSA web site at http://www.minsocam.org, go to the American Mineralogist Contents, find the table of contents for the specific volume/issue wanted, and then click on the deposit link there.

TABLE 2. Atomic coordinates (x10^4) and equivalent isotropic displacement parameters (Å^2 x 10^3) for *m* = 16 antigorite Mg159

	x	y	z	U_{eq}		x	y	z	U_{eq}		x	y	z	U_{eq}
T1	9849(1)	8335(1)	8676(2)	21(1)	B7B	7798(1)	7416(4)	9235(7)	43(1)	W3B	9118(1)	6707(11)	2841(9)	28(2)
T2	9534(1)	6664(1)	8275(2)	21(1)	B8B	7500	7500	10000	63(3)	W4A	8781(1)	5000	2740(16)	25(4)
T3	9216(1)	8336(1)	8059(2)	20(1)	M1A	10000	10000	5000	19(2)	W4B	8780(1)	8305(11)	2807(8)	23(2)
T4	8895(1)	6664(1)	7958(2)	21(1)	M1B	10000	6649(8)	5000	20(1)	W5A	8449(1)	10000	2820(16)	26(3)
T5	8574(1)	8336(1)	7942(2)	21(1)	M2A	9668(1)	5000	4629(8)	19(2)	W5B	8442(1)	6674(12)	2794(8)	23(2)
T6	8254(1)	6664(1)	8015(2)	22(1)	M2B	9665(1)	8337(6)	4598(4)	20(1)	W6A	8104(1)	5000	2952(15)	22(3)
T7	7938(1)	8336(1)	8237(2)	24(1)	M3A	9332(1)	10000	4301(8)	19(2)	W6B	8107(1)	8318(11)	2966(8)	25(2)
T8	7619(1)	6665(1)	8626(2)	25(1)	M3B	9334(1)	6648(6)	4308(4)	20(1)	W7A	7765(1)	10000	3198(15)	28(3)
A1	9881(1)	8303(11)	6491(8)	26(2)	M4A	9003(1)	5000	4165(8)	18(2)	W7B	7765(1)	6697(11)	3307(8)	24(2)
A2	9550(1)	6637(10)	6071(7)	18(2)	M4B	9001(1)	8316(6)	4160(4)	18(1)	I1	9882(1)	5000	7720(60)	23(9)
A3	9217(1)	8321(11)	5841(8)	21(2)	M5A	8669(1)	10000	4116(8)	20(2)	I2	9538(1)	10000	7370(60)	23(9)
A4	8893(1)	6686(11)	5712(8)	26(2)	M5B	8671(1)	6658(6)	4113(4)	17(1)	I3	9228(1)	5000	7040(60)	23(9)
A5	8569(1)	8392(10)	5733(8)	22(2)	M6A	8338(1)	5000	4126(8)	23(2)	I4	8894(1)	10000	7000(60)	23(9)
A6	8238(1)	6713(10)	5799(8)	22(2)	M6B	8337(1)	8337(6)	4181(4)	18(1)	I5	8559(1)	5000	6920(60)	23(9)
A7	7909(1)	8345(10)	6026(7)	21(2)	M7A	8005(1)	10000	4301(8)	18(2)	I6	8239(1)	10000	7030(60)	23(9)
A8	7575(1)	6681(11)	6474(7)	27(2)	M7B	8003(1)	6662(6)	4396(4)	23(1)	I7	7910(1)	5000	7340(60)	23(9)
B1A	9807(1)	10000	9391(9)	35(2)	M8A	7669(1)	5000	4812(8)	21(1)	I8	7570(1)	10000	7560(60)	23(9)
B2A	9511(1)	5000	9048(8)	28(2)	M8B	7668(1)	8346(4)	4727(4)	21(1)	H1A	9785(1)	10000	2040(70)	47(6)
B3A	9207(1)	10000	8852(8)	32(2)	V1	9882(1)	5000	6385(14)	19(3)	H1B	9788(1)	6700(10)	1910(50)	47(6)
B4A	8887(1)	5000	8720(8)	30(2)	V2	9538(1)	10000	6049(16)	31(3)	H2A	9461(1)	5000	1810(70)	47(6)
B5A	8564(1)	10000	8736(8)	32(2)	V3	9228(1)	5000	5787(15)	22(3)	H2B	9447(1)	8360(10)	1680(50)	47(6)
B6A	8246(1)	5000	8819(9)	33(2)	V4	8894(1)	10000	5689(15)	18(3)	H3A	9109(1)	10000	1490(70)	47(6)
B7A	7934(1)	10000	9053(9)	34(2)	V5	8559(1)	5000	5611(14)	20(3)	H3B	9118(1)	6707(11)	1410(50)	47(6)
B8A	7631(1)	5000	9484(11)	61(2)	V6	8239(1)	10000	5777(16)	24(3)	H4A	8781(1)	5000	1350(70)	47(6)
B0B	10000	7778(6)	10000	27(2)	V7	7910(1)	5000	6051(16)	34(4)	H4B	8780(1)	8305(11)	1470(50)	47(6)
B1B	9697(1)	7333(4)	9266(6)	25(1)	V8	7570(1)	10000	6248(12)	19(3)	H5A	8449(1)	10000	1380(70)	47(6)
B2B	9379(1)	7590(4)	8992(6)	21(1)	W1A	9785(1)	10000	3453(16)	33(4)	H5B	8442(1)	6674(12)	1410(50)	47(6)
B3B	9060(1)	7438(4)	8815(6)	23(1)	W1B	9788(1)	6700(10)	3412(7)	18(2)	H6A	8104(1)	5000	1520(70)	47(6)
B4B	8741(1)	7570(4)	8730(6)	24(1)	W2A	9461(1)	5000	3092(16)	34(4)	H6B	8107(1)	8318(11)	1640(50)	47(6)
B5B	8423(1)	7412(4)	8769(6)	24(1)	W2B	9447(1)	8360(10)	3059(7)	19(2)	H7A	7765(1)	10000	1570(70)	47(6)
B6B	8107(1)	7602(4)	8909(6)	30(1)	W3A	9109(1)	10000	2888(14)	15(3)	H7B	7765(1)	6697(11)	1920(60)	47(6)

Notes: U_{eq} is defined as one third of the trace of the orthogonalized U_{ij} tensor. T = tetrahedral Si atoms; A = apical tetrahedral O atoms; B = basal tetrahedral O atom (A = on mirror plane; B = not on mirror plane); M = octahedral Mg atoms (A = in special position; B = in general position); V = internal hydroxyl O atom; W = external hydroxyl O atom (A = in special position; B = in general position); I = internal hydrogen atoms (linked to V); H = external hydrogen atoms (linked to W).

by 2-diad and 2_1-screw axes in the *m* = 16 polysome. Conversely, the rotational symmetry is disrupted in the *m* = 17 polysome, because of the presence of an extra-module that leads to symmetry-unrelated half-waves ("short" and "long" half-waves). Diad and screws survive only as local symmetry operators in the *m* = 17 polysome. Because of the ½(**a**+**b**) translation owing to the *C*-centering, the [010] projection shows an apparent halved [100] periodicity.

Whereas the [010] projection emphasizes the similarities, the [001] projection displays the major differences between the *m* = 16 and *m* = 17 antigorite polysomes (cf., Fig. 2 with Fig. 2 in Capitani and Mellini 2004). As in the *m* = 17 polysome, alternating 6-reversals and 8-reversals occur in the **T**-sheet of the *m* = 16 polysome. However, whereas the reversals are repeated by a *P* lattice in the *m* = 17 polysome, they are repeated by a *C*-centered lattice in the *m* = 16 polysome. In other words, in the *m* = 16 polysome, 8-reversals and 4-reversals exchange their positions from one wave to an adjacent wave. Consequently, two nearby 6-reversals reverse their polarities. Therefore, the refined structure of the *m* = 16 polysome matches also the proposal by Uehara and Shirozu (1985) better than any other previous model.

Bond geometry

Both the M-O and T-O bonding patterns of the *m* = 16 antigorite polysome closely match the corresponding bonding patterns determined for the *m* = 17 polysome. In particular, most of the M sites (Table 3) maintain the same coordination as in lizardite, consisting of three W hydroxyls (see Table 2 for site designations) located on the outer convex surface, one V hydroxyl located on the inner concave surface, and two A oxygen atoms shared with silicon tetrahedra. At the 6-reversal, M8A is connected to four hydroxyl groups, but M8B is connected to only three. At the 8-reversal, M1B is connected to four hydroxyl groups, but M1A is connected to only two. Taking into account site multiplicities, we conclude that four and two hydrogen atoms are omitted at the 6- and 8-reversals, respectively.

The M octahedra (actually, trigonal antiprisms) have <M-O> average bond distance of 2.091 Å (vs. 2.088 Å in the *m* = 17 polysome), individual bond distances ranging from 2.002 to 2.210 Å (vs. 2.005 to 2.207 Å), average M-W of 2.048 Å (vs. 2.047 Å), average M-V of 2.109 Å (vs. 2.118 Å), average M-A of 2.136 Å (vs. 2.126 Å). Therefore, the M-O bonding pattern of the *m* = 16 antigorite is nearly indistinguishable from the bonding pattern of lizardite (as detailed in Capitani and Mellini 2004). The tetrahedral T-O bond distances (Table 4) range from 1.595 to 1.668 Å (vs. 1.553 to 1.686 in the *m* = 17 polysome), with the average T-A apical bond distance being systematically shorter than the T-B basal bond distance (1.614 and 1.634 Å, respectively, vs. 1.617 and 1.637 Å in *m* = 17). The bonding pattern of the **T**-sheet in antigorite again matches the bonding pattern of the **T**-sheet in lizardite (1.615 and 1.645 Å; Mellini and Viti 1994). In conclusion, the polyhedral geometry does not show any major difference, either when two different antigorite polysomes are compared, or when antigorite is compared with lizardite.

Thickness of the T- and O-sheet

Previous authors have used the sheet thickness for comparison of the crystal structures of serpentine minerals (e.g., Wicks and O'Hanley 1988). It therefore seems useful to comment on the

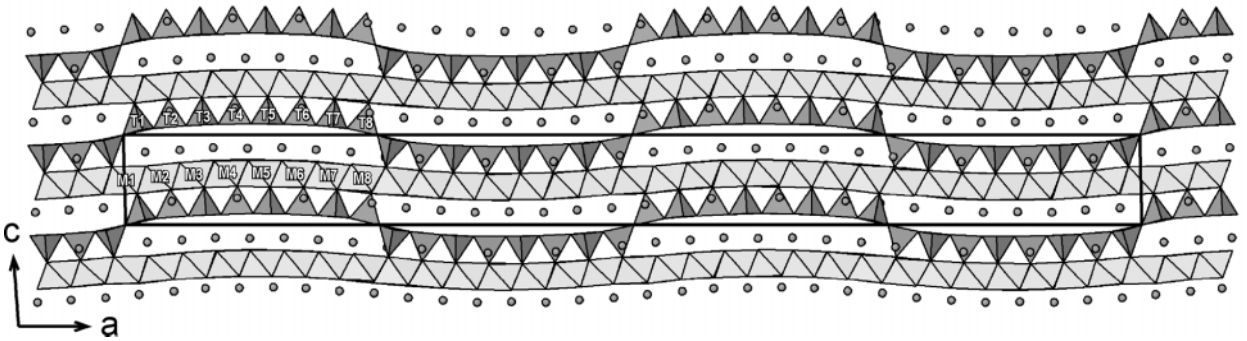

FIGURE 1. [010] projection of the modulated structure of the *C*-centered *m* = 16 antigorite. As in the *m* = 17 polysome, the **T**-sheet links at the concave side of the continuous **O**-sheet. Circles represent hydrogen atoms. Adjacent half-waves along [100] are symmetry-related through alternating 2 and 2_1 axes. The [010] projection shows a halved *a* periodicity because of the **b**/2 shift between adjacent waves.

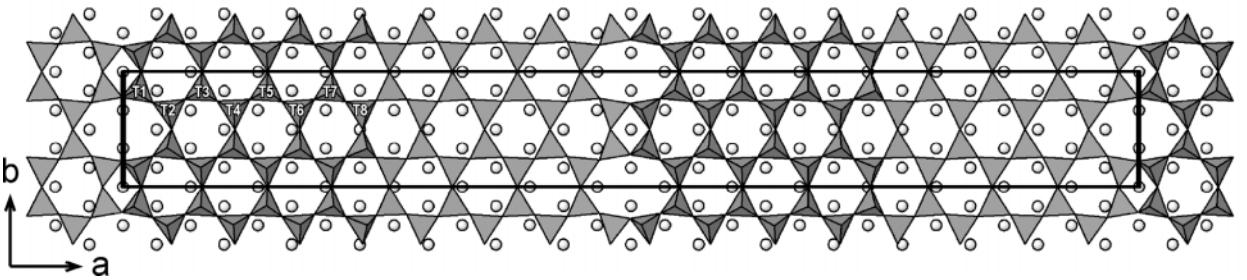

FIGURE 2. [001] projection of the *C*-centered *m* = 16 antigorite structure. For clarity, only the **T**-sheet and the octahedral Mg sites (circles) are depicted. The **T**-sheet reverses polarity every eight tetrahedra, at 6- and 8-reversals, through 2-diad axes at *x* = 0 and *x* = 1/2, and 2_1 screw axes at *x* = 1/4 and 3/4.

TABLE 3. Mg-O bond distances (in angstroms) for the *m* = 16 antigorite Mg159 (e.s.d. in brackets)

M1A-W1A	2.060(11)	M1B-W1B	2.056(5)	M2A-W2A	2.002(11)	M2B-W1A	2.016(8)
M1A-W1A	2.060(11)	M1B-W1B	2.056(5)	M2A-W1B	2.064(8)	M2B-W1B	2.022(9)
M1A-A1	2.153(8)	M1B-V1	2.076(8)	M2A-W1B	2.064(8)	M2B-W2B	2.075(5)
M1A-A1	2.153(8)	M1B-V1	2.076(8)	M2A-A2	2.090(8)	M2B-A2	2.133(9)
M1A-A1	2.153(8)	M1B-A1	2.124(10)	M2A-A2	2.090(8)	M2B-V2	2.145(8)
M1A-A1	2.153(8)	M1B-A1	2.124(10)	M2A-V1	2.139(11)	M2B-A1	2.210(6)
M3A-W2B	2.011(8)	M3B-W3B	2.042(6)	M4A-W4A	2.069(12)	M4B-W3B	2.021(10)
M3A-W2B	2.011(8)	M3B-W2B	2.057(9)	M4A-W3B	2.082(9)	M4B-W3A	2.025(7)
M3A-W3A	2.069(11)	M3B-W2A	2.057(8)	M4A-W3B	2.082(9)	M4B-W4B	2.039(6)
M3A-V2	2.083(12)	M3B-V3	2.069(8)	M4A-A4	2.134(9)	M4B-A4	2.091(10)
M3A-A3	2.145(9)	M3B-A3	2.144(9)	M4A-A4	2.134(9)	M4B-V4	2.116(8)
M3A-A3	2.145(9)	M3B-A2	2.155(6)	M4A-V3	2.154(12)	M4B-A3	2.120(6)
M5A-W5A	2.005(12)	M5B-W4B	2.014(10)	M6A-W5B	2.027(9)	M6B-W5B	2.040(10)
M5A-W4B	2.055(9)	M5B-W4A	2.049(8)	M6A-W5B	2.027(9)	M6B-W5A	2.055(8)
M5A-W4B	2.055(9)	M5B-W5B	2.074(6)	M6A-W6A	2.072(11)	M6B-W6B	2.060(6)
M5A-A5	2.076(9)	M5B-V5	2.101(8)	M6A-V5	2.083(11)	M6B-A6	2.086(9)
M5A-A5	2.076(9)	M5B-A4	2.133(6)	M6A-A6	2.170(9)	M6B-V6	2.099(8)
M5A-V4	2.142(11)	M5B-A5	2.168(9)	M6A-A6	2.170(9)	M6B-A5	2.178(6)
M7A-W6B	2.024(9)	M7B-W6A	2.045(8)	M8A-W7B	2.076(9)	M8B-W7B	2.015(9)
M7A-W6B	2.024(9)	M7B-W6B	2.046(10)	M8A-W7B	2.076(9)	M8B-V8	2.061(7)
M7A-W7A	2.096(11)	M7B-W7B	2.082(6)	M8A-V8	2.084(10)	M8B-W7A	2.061(8)
M7A-A7	2.140(8)	M7B-V7	2.104(9)	M8A-A8	2.124(9)	M8B-A8	2.145(9)
M7A-A7	2.140(8)	M7B-A7	2.114(9)	M8A-A8	2.124(9)	M8B-A8	2.150(6)
M7A-V6	2.170(12)	M7B-A6	2.146(6)	M8A-V7	2.143(12)	M8B-A7	2.159(6)
<M-O>	2.091(49)	<M-W>	2.048(24)	<M-V>	2.109(33)	<M-A>	2.136(30)

sheet thickness for this newly determined structure. The *m* = 16 antigorite polysome has a **T**-sheet thickness (Table 5) ranging from 2.186 to 2.302 Å, in agreement with the 2.162 and 2.307 Å values of the *m* = 17 structure. The **O**-sheet thickness (Table 6) was calculated at different locations within the layer, by considering the least-squares planes through oxygen atoms on opposite sides of the sheet. Values range from 2.100 to 2.172 Å, vs. 2.057 to 2.159 Å in *m* = 17 antigorite and 2.10 to 2.12 Å in lizardite.

The major distortion obviously occurs close to the tetrahedral reversals. If the M1 and M8 polyhedra are excluded, the range reduces to 2.100–2.115 Å. In contrast, distortion at reversal lines matches expectations. On the other hand, details of these distortion patterns, because the refined values may be biased by polysomatic faults that locally displace the reversal lines, are considered tentative.

Curvature radii and modulation amplitude

The 1:1 layer modulation may be analyzed either in terms of curvature radius (e.g., Wicks and O'Hanley 1988; Grobéty 2003) or in terms of modulation amplitude (Capitani and Mellini 2004). For the *m* = 16 polysome, a unique curvature radius of 80.1 Å was calculated using a surface passing through M2, M5, and M8. This value is lower than in the *m* = 17 polysome (99.4 and 110.9 Å, for the long and short half waves, respectively), whereas the subtended angle (14.4°) is larger (13.3 and 10.6°).

TABLE 4. Si-O bond distances (in angstroms) for the *m* = 16 antigorite Mg159 (e.s.d. in brackets)

T1-A1	1.614(6)	T5-A5	1.605(6)
T1-B1B	1.617(4)	T5-B5B	1.628(4)
T1-B0B	1.625(2)	T5-B4B	1.630(4)
T1-B1A	1.666(3)	T5-B5A	1.647(3)
T2-A2	1.609(5)	T6-A6	1.612(6)
T2-B1B	1.622(4)	T6-B5	1.622(4)
T2-B2B	1.624(4)	T6-B6	1.632(4)
T2-B2A	1.651(3)	T6-B6A	1.649(3)
T3-A3	1.611(6)	T7-B6B	1.606(4)
T3-B3B	1.626(4)	T7-B7B	1.608(5)
T3-B2B	1.633(4)	T7-A7	1.617(6)
T3-B3A	1.646(3)	T7-B7A	1.651(3)
T4-B4B	1.622(4)	T8-A8	1.595(5)
T4-A4	1.631(6)	T8-B8B	1.609(2)
T4-B3B	1.637(4)	T8-B8A	1.664(3)
T4-B4A	1.638(2)	T8-B7B	1.668(5)
<T-O>	1.629(19)	<T-A>	1.614(12)
		<T-B>	1.634(18)

TABLE 5. Thickness (in angstroms) of the tetrahedral sheet modules (e.s.d. in brackets) for the *m* = 16 antigorite Mg159

T1	2.264	(7)	T5	2.186	(7)
T2	2.211	(6)	T6	2.205	(7)
T3	2.211	(6)	T7	2.220	(7)
T4	2.209	(7)	T8	2.302	(7)

TABLE 6. *m* = 16 antigorite Mg159; thickness (in angstroms) of the octahedral sheet modules (central columns) and distances of the Mg atoms to the planes through the internal (left columns) and external (right columns) O atoms, respectively (e.s.d. in brackets)

1.098	(6)	M1A	1.098	(6)	0.949	(9)	M5A	1.163	(8)
1.073	(4)	M1B	1.073	(4)	0.970	(5)	M5B	1.132	(5)
		2.172	(43)				2.107	(22)	
0.968	(8)	M2A	1.131	(7)	0.928	(8)	M6A	1.175	(8)
0.937	(5)	M2B	1.164	(5)	0.957	(6)	M6B	1.148	(5)
		2.100	(20)				2.104	(23)	
0.946	(8)	M3A	1.172	(8)	0.910	(8)	M7A	1.197	(8)
0.951	(6)	M3B	1.151	(5)	0.968	(5)	M7B	1.139	(6)
		2.110	(22)				2.107	(22)	
0.982	(8)	M4A	1.143	(8)	1.004	(8)	M8A	1.105	(8)
0.955	(5)	M4B	1.148	(5)	1.005	(5)	M8B	1.097	(5)
		2.115	(23)				2.105	(38)	

The modulation amplitude is approximately 0.51 Å (calculated using the average *z* coordinate of T4 and T5, with respect to the average *z* coordinate of T1 and T8). This unique value falls in the range 0.46–0.56 Å of the *m* = 17 polysome. Therefore, all the values resulting from the refined structures are internally consistent, and differ from the 36 Å curvature radius and the 2.18 Å modulation amplitude estimated from HRTEM images by Dodony et al. (2002).

Again, structural modulation in antigorite produces deformation patterns that are similar to chrysotile (reversals apart). For instance, the different quantitative estimates of the curvature radii (80.1, 99.4, and 110.9 Å) match both the ideal radius of 88 Å (Wicks and Whittaker 1975) and the TEM observations indicating maximum outer radius close to 135–140 Å.

Ditrigonalization and O-O distances

Table 7 reports the angles among basal oxygen atoms within different tetrahedral rings, together with the α-values used to characterize the entity of ditrigonalization in the *m* = 16 polysome. These values range between –5.8 and –11.7°, and compare to –4.0 and –13.6° for the *m* = 17 polysome. Table 8 reports the interlayer O-O distances, which vary from 2.958 to 3.343 Å and are comparable with the values of the *m* = 17 polysome (2.860 to 3.421 Å). Therefore, also the new determination indicates the absence of a homogeneous, continuous interlayer hydrogen-bonding network.

DISCUSSION

The complex structural modulation of antigorite may be described as longitudinal and transverse modulations. The transverse modulation derives from the wave-shaped 1:1 layer, and the longitudinal modulation from the periodical inversion of the **T**-sheet through alternating 6- and 8-reversals. Refinements are available only for the *m* = 16 and *m* = 17 polysomes, based upon waves with lengths of ~40.8 and ~43.5 Å, respectively. However, extensive electron diffraction data show wavelength

TABLE 8. Inter-layer O-O distances (in angstroms) for the *m* = 16 antigorite Mg159 (e.s.d. in brackets)

W1A-B1A	2.958(14)	W1B-B1B	3.138(7)
W2A-B2A	2.975(13)	W2B-B2B	3.076(7)
W3A-B3A	3.055(12)	W3B-B3B	3.026(8)
W4A-B4A	3.065(13)	W4B-B4B	3.046(8)
W5A-B5A	3.132(13)	W5B-B5B	3.002(8)
W6A-B6A	3.245(13)	W6B-B6B	3.020(8)
W7A-B7A	3.343(13)	W7B-B7B	3.050(8)

TABLE 7. *m* = 16 antigorite Mg159: angles (°) among the basal tetrahedral O atoms (e.s.d. in brackets) and α-values (right column) of the related ditrigonal distortion for the lizardite-type 6-membered rings (L1 to L6) and 6-reversal (α defined as the average deviation from 120°)

4-rev.	B1A-B0B-B1A	76.8(3)	B0B-B1A-B0B	103.2(3)						-13.2
8-rev.	B1B-B0B-B1B	161.4(3)	B0B-B1B-B2A	134.2(2)	B1B-B2A-B1B	109.6(3)				-13.4
L1	B1B-B1A-B1B	140.1(3)	B2B-B1B-B1A	104.7(2)	B1B-B2B-B3A	127.5(2)	B2B-B3A-B2B	115.4(3)		-11.7
L2	B2B-B2A-B2B	131.5(3)	B3B-B2B-B2A	111.1(2)	B2B-B3B-B4A	125.2(2)	B3B-B4A-B3B	115.7(3)		-7.3
L3	B3B-B3A-B3B	126.4(3)	B4B-B3B-B3A	114.1(2)	B3B-B4B-B5A	125.4(2)	B4B-B5A-B4B	114.5(3)		-5.8
L4	B4B-B4A-B4B	126.9(3)	B5B-B4B-B4A	113.4(2)	B4B-B5B-B6A	126.1(2)	B5B-B6A-B5B	114.3(3)		-6.3
L5	B5B-B5A-B5B	128.6(3)	B6B-B5B-B5A	111.8(2)	B5B-B6B-B7A	126.5(2)	B6B-B7A-B6B	114.8(3)		-7.2
L6	B6B-B6A-B6B	129.3(3)	B7B-B6B-B6A	111.4(2)	B6B-B7B-B8A	125.6(2)	B7B-B8A-B7B	116.5(3)		-6.9
6-rev.	B7B-B7A-B7B	129.8(3)	B8B-B7B-B7A	113.2(2)	B7B-B8B-B8A	117.8(2)	B8B-B8A-B8B	127.5(3)		-5.9

Note: Analogous distortion parameters, defined as the average deviation from 90° and 135°, are given for the 8-membered ring (8-rev.) and the 4-membered ring (4-rev.), respectively.

values from 33 to 61 Å (as reported in Capitani and Mellini 2005), namely from m = 13 to m = 24. The m value is an important crystal-chemical parameter, because it directly relates the chemical composition through the polysomatic formula of $Mg_{3m-3}Si_{2m}O_5(OH)_{4m-6}$.

However, we note that the m value is not coincident with the a periodicity. In fact, our data match the proposal by Uehara and Shirozu (1985) of two different basic antigorite variants. Following Capitani and Mellini (2005), we propose that "odd" antigorites with $m = 2n + 1$ (as in the case of the refined m = 17 structure) have Pm space group, and the m number of tetrahedra within a wave coincides with the m number of tetrahedra along **a**. Conversely, "even" antigorites with $m = 2n$ (as in the case of the present m = 16 structure) have $C2/m$ space group, still with m tetrahedra within each wave, but two waves (and 2m tetrahedra) along **a**. Alternating 6-reversals and 8-reversals do occur in both the antigorite variants, which differ from the model of Dodony et al. (2002) with only 6-reversals.

The structural analysis of the m = 17 polysome (Capitani and Mellini 2004) left unresolved the issue of the nature of the reversals for even polysomes because no refinements were available. Previous and present data definitely demonstrate the occurrence of 6- and 8-reversals, at least in the m = 16 and m = 17 polysomes. We extend this conclusion to all the m even and m odd antigorite 1:1 layers, as supported by the numerous HRTEM evidences pointing to the presence of 8-reversals in antigorite with variable wavelengths (e.g., Wu et al. 1989; Uehara 1998; Grobéty 2003; Capitani and Mellini 2005, and in preparation).

However, the previously described P and C structures do not exhaust the range of possible structures. As already observed (e.g., Veblen 1980; Otten 1993; Grobéty 2003; Dodony et al. 2002; Capitani and Mellini 2005) defects in antigorite also include (001) polysynthetic twins, (001) polytypic variants, and mixed-ordered polysomes. Not all of these structures are equally probable. Current diffraction data and HRTEM observations seem to indicate that the most common m values cluster around m = 17.

Acknowledgments

We renew our thanks to A. Peretti for the careful separation of the Mg159 antigorite crystals. G.C.C. is indebted to C. Paulmann for his invaluable aid with the F1 beamline at Desy. S. Guggenheim and S. Uehara are greatly acknowledged for their valuable reviews.

References cited

Altomare, A., Burla, M.C., Camalli, M., Cascarano, G., Giacovazzo, C., Guagliardi, A., Moliterni, A.G.G., Polidori, G., and Spagna, R. (1999) Sir97: A new tool for crystal structure determination and refinement. Journal of Applied Crystallography, 32, 115–119.

Capitani, G.C. and Mellini, M. (2004) The modulated crystal structure of antigorite: the m = 17 polysome. American Mineralogist, 89, 147–158.

——— (2005) HRTEM evidence for 8-reversals in the m = 17 antigorite polysome. American Mineralogist, 90, 991–999.

Dodony, I., Posfài, M., and Buseck, P.R. (2002) Revised structure models for antigorite: An HRTEM study. American Mineralogist, 87, 1443–1457.

Grobéty, B. (2003) Polytypes and higher-order structures of antigorite: A TEM study. American Mineralogist, 88, 27–36.

Kunze, V.G. (1958) Die gewellte Struktur des Antigorits, II. Zeitschrift für kristallographie, 110, 282–320.

——— (1961) Antigorit. Fortschritte der Mineralogie, 39, 206–324.

Mellini, M. and Viti, C. (1994) Crystal structure of lizardite-1T from Elba, Italy. American Mineralogist, 79, 1194–1198.

Mellini, M., Trommsdorff, V., and Compagnoni, R. (1987) Antigorite polysomatism: Behaviour during progressive metamorphism. Contributions to Mineralogy and Petrology, 97, 147–155.

Otten, M.T. (1993) High-resolution electron microscopy of polysomatism and stacking defects in antigorite. American Mineralogist, 78, 75–84.

Peretti, A. (1988) Occurrence and stability of opaque minerals in the Malenco serpentinite, 182 p. Ph.D. Dissertation, ETH, Zurich.

Robinson, K. and Shaw, E.R.S. (1952) Summarized proceedings of a conference on structures of silicate minerals—London November 1951. British Journal of Applied Physics, 3, 277–282.

Sheldrick, G.M. (1996) SADABS, Siemens area detector absorption correction software. University of Göttingen, Germany.

——— (1997) SHELXL-97, A program for crystal structure refinement. University of Göttigen, Germany, release 97–2.

Spinnler, G.E. (1985) HRTEM study of antigorite, pyroxene-serpentine reactions and chlorite, 248 p. Ph.D. Thesis, Arizona State University, Tempe, Arizona.

Uehara, S. (1998) TEM and XRD study of antigorite superstructures. Canadian Mineralogist, 36, 1595–1605.

Uehara, S. and Shirozu, H. (1985) Variations in chemical composition and structural properties of antigorites. Mineralogical Journal, 12, 299–318.

Veblen, D.R. (1980) Anthophyllite asbestos: microstructure, intergrown sheet silicates, and mechanism of fiber formation. American Mineralogist, 65, 1075–1086

Viti, C. and Mellini, M. (1996) Vein antigorite from Elba Island, Italy. European Journal of Mineralogy, 8, 423–434.

Wicks, F.J. and O'Hanley, F.C. (1988) Serpentine minerals: Structures and petrology. In S.W. Bailey, Ed., Hydrous Phyllosilicates (exclusive of micas), 19, 91–159. Reviews in Mineralogy, Mineralogical Society of America, Chantilly, Virginia.

Wicks, F.J. and Whittaker, E.J.W. (1975) A reappraisal of the structures of the serpentine minerals. Canadian Mineralogist, 13, 227–243.

Wu, X.J., Li, F.H., and Hashimoto, H. (1989) High-resolution transmission electron microscopy study of the superstructure of Xiuyan Jade and Matterhorn serpentine. Acta Crystallographica, B45, 129–136.

Manuscript received February 16, 2005
Manuscript accepted May 3, 2005
Manuscript handled by Stephen Guggenheim